

## DIAGNOSTICS OF PLASMA INDUCED IN Nd:YAG LASER WELDING OF ALUMINUM ALLOY

by Jong-Do Kim<sup>1\*</sup>, Myeong-Hoon Lee<sup>1</sup>, Young-Sik Kim<sup>1</sup>,  
Seiji Katayama<sup>2</sup> and Akira Matsunawa<sup>2</sup>

<sup>1</sup> Division of Marine Engineering System, Korea Maritime University  
Dongsam-Dong, Youngdo-Gu, Busan 606-791, Korea, jdkim@hanara.kmaritime.ac.kr

<sup>2</sup> Welding Research Institute, Osaka University  
11-1 Mihogaoka, Ibaraki, Osaka 567, Japan, katayama@jwri.osaka-u.ac.jp

### ABSTRACT

The dynamic behavior of Al-Mg alloys plasma was very unstable and this instability was closely related to the unstable motion of keyhole during laser irradiation. The keyhole fluctuated both in size and shape and its fluctuation period was about 440  $\mu\text{m}$ . This instability has been estimated to be caused by the evaporation phenomena of metals with different boiling point and latent heats of vaporization. Therefore, the authors have conducted the spectroscopic diagnostics of plasma induced in the pulsed YAG laser welding of Al-Mg alloys in air and argon atmospheres. In the air environment, the identified spectra were atomic lines of Al, Mg, Cr, Mn, Cu, Fe and Zn, and singly ionized Mg line, as well as strong molecular spectrum of AlO, MgO and AlH. It was confirmed that the resonant lines of Al and Mg were strongly self-absorbed, in particular in the vicinity of pool surface. The self-absorption of atomic Mg line was more eminent in alloys containing higher Mg. These facts showed that the laser-induced plasma was relatively a low temperature and high density metallic vapor. The intensities of molecular spectra of AlO and MgO were different each other depending on the power density of laser beam. Under the low power density irradiation condition, the MgO band spectra were predominant in intensity, while the AlO spectra became much stronger in higher power density. In argon atmosphere the band spectra of MgO and AlO completely vanished, but AlH molecular spectra was detected clearly. The hydrogen source was presumably the hydrogen solved in the base Metal, absorbed water on the surface oxide layer or H<sub>2</sub> and H<sub>2</sub>O in the shielding gas. The temporal change in spectral line intensities was quite similar to the fluctuation of keyhole. The time average plasma temperature at 1 mm high above the surface of A5083 alloy was determined by the Boltzmann plot method of atomic Cr lines of different excitation energy. The obtained electron temperature was  $3,280 \pm 150$  K which was about 500 K higher than the boiling point of pure aluminum. The electron number density was determined by measuring the relative intensities of the spectral lines of atomic and singly ionized Magnesium, and the obtained value was  $1.85 \times 10^{19} \text{ 1/m}^3$ .

### 1. Introduction

It is widely known that evaporation from the weld pool plays the most important role to achieve the deep penetration in laser welding. A deep keyhole is made by the recoil pressure of vaporization which is balanced with gravity head of molten pool and surface tensional pressure. A keyhole is mainly filled by metal vapor, but its physical properties such as temperature, density, velocity and so on are not well known. It has been observed by the present authors that the key-hole fluctuates very quickly in random way and its instability, especially at the time of solidification, is closely related to the formation of porosity<sup>1)</sup>. The instability of keyhole is also reflected to the plasma behavior above the specimen surface<sup>1)</sup>. Therefore, the keyhole behavior and its inner state can be estimated if the plasma behavior is carefully observed and analyzed. As well known, the plasma absorbs and scatters the incident laser beam energy and the energy coupling with materials is affected by the plasma behavior<sup>2)</sup>.

However, evaporation phenomena and characteristics of laser induced plasma of alloys containing large amount of volatile elements have not been understood. The authors, therefore, conducted the spectroscopic analyses of the pulsed YAG laser induced plasma of Al-Mg alloys in air argon atmosphere together with the direct observation of key-hole in order to clarify the beam-matter interaction during laser welding.

### 2. Experimental procedures

#### 2.1 Materials used

Al-Mg alloys used in this study are tabulated in Table 1, and the major physical constants of pure Al and Mg are listed in Table 2.

Table 1 Chemical composition of commercially available Aluminum alloys

Al alloy	Plate thickness (mm)	Chemical composition (mass%)								
		Si	Fe	Cu	Mn	Mg	Cr	Zn	Ti	Al
A5083P-O	6	0.14	0.22	0.04	0.70	4.58	0.12	0.01	0.02	Bal.
A5182P-O	7	0.08	0.23	0.03	0.29	4.55	0.03	0.01	0.01	Bal.
A5052P-O	6	0.08	0.27	0.01	0.00	2.69	0.18	0.00	-	Bal.
A7N01S-T5	6	0.07	0.14	0.08	0.44	1.18	0.21	4.74	0.03	Bal.
A6061P-T6	6	0.57	0.42	0.20	0.04	1.03	0.25	0.15	0.03	Bal.

Table 2 Physical constants of pure Aluminum and Magnesium<sup>3,4)</sup>

	Atomic number	Atomic weight	Melting point [K]	Boiling point [K]	Ionization potential [eV]	Heat of fusion [ $10^3$ J/mole]	Heat of vaporization [ $10^3$ J/mole]	Thermal conductivity (at 293 K) [W/m·K]
Pure Al	13	26.9815	933.25	2750±50	5.984	8.40±0.16	293.8	238
Pure Mg	12	24.305	932±0.5	1376±5	7.644	8.96±0.2	128.7	167

## 2.2 Pulsed Nd:YAG laser

A pulsed shapable YAG laser (Miyachi Technos: Model MHL250A) was used in this study. The overall pulse duration was able to change from 1 to 21 ms, and the pulse duration was divided into 20 time-segments and the energy in each time-segment could change. Thus, the pulse shape was possible to change quite freely. the total maximum energy was 90 J/pulse. The beam was delivered by the 600 $\mu$ m GI fiber and focused on the specimen by the quartz lens of 150 mm focal length.

## 2.3 Optical system for spectroscopic analysis

A 500 mm Czerny-Turner type double monochromator was used for spectrophotographic and photoelectric photometries. A grating with 2400grooves/mm (blaze wave length: 240 nm) was used, and the measurements were conducted in the wave length range of 200-900 nm with the resolution of 0.02 nm at 10  $\mu$ m slit width. Figure 1 shows the schematic diagram of optical arrangements for spectroscopic measurement. The laser induced plasma was focused by a specially compensated lens for chromatic aberration. The image of plasma was introduced to the 40 optical fibers(diameter: 200  $\mu$ m, N.A.:0.2)which was bundled linearly in order to obtain the spatial distribution of light intensity. The another end of the bundled of fiber were connected to a special optics shown (B) in Figure1 which could compensate astigmatism. In photoelectric photometry, a multi-channel photo detector (Hamamatsu photonics: Model PMA-50) was used and signals were analyzed by a wave analyzer (Max. data processing rate: 100 kHz).

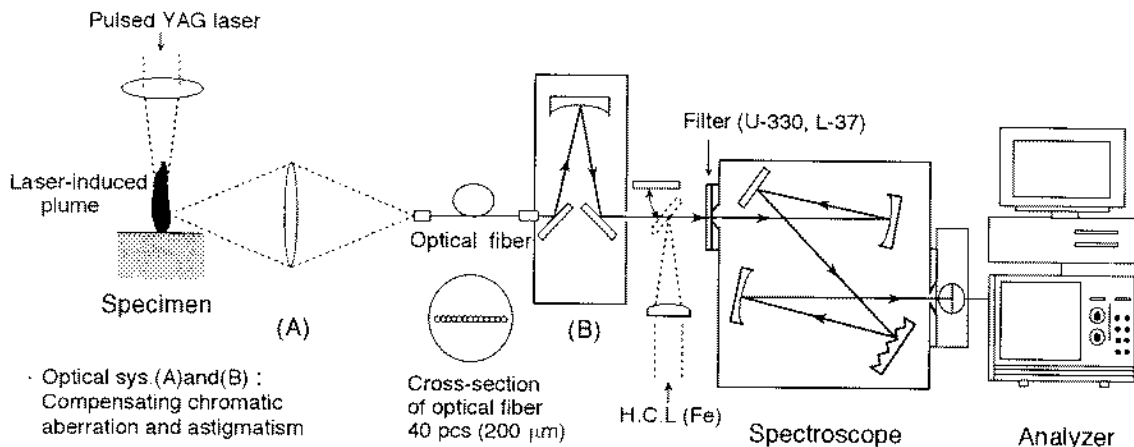


Fig.1 Schematic diagram of optical arrangements for spectroscopic measurement

3. Results and Discussion

3.1 Identification of emission spectral lines and their features

Identification of spectrum<sup>5,6)</sup> was carried out by a Fe-hollow cathode lamp(H.C.L.(Fe)). The shift of focal point by chromatic aberration was carefully adjusted in the wavelength range of 250-600 nm by using a Hg lamp.

Figure 2 shows a typical example of spectrum photograph where the right side is the H.C.L.(Fe) spectral lines and the left is the spectra emitted from A5083 laser plasma. The vertical striations in the picture correspond to each optical fiber of 40 bundled cable and thus the lateral intensity of spectral line corresponds to the lateral distribution of emission. The lines marked by \* are the persistent spectra<sup>7)</sup>. The identified spectral lines were the atomic spectra of Mg, Mn and Al, and singly ionized lines of Mg(279.553 and 280.270 nm) were detected. It was clearly seen in Figure 2(a) and (b) that atomic lines of Al and Mg showed black lines at the center and these lines were strongly self-absorbed. In particular, the self-absorption of Mg lines was predominant. The transition energies of these spectra showed that the lower energy level was in the ground state or close to it.<sup>8,9)</sup> As the degree of self-absorption was not clear in the photograph, the authors conducted precise measurements of photoelectric photometries, and the results were presented in Figure 3(a) and (b).

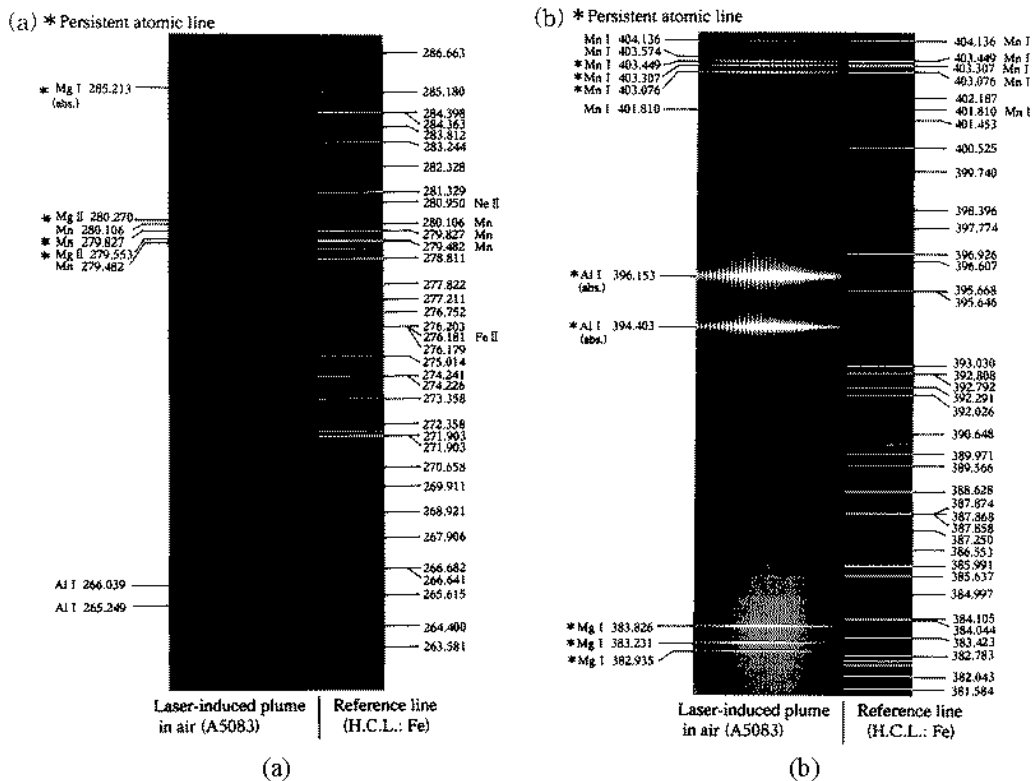


Fig.2 Atomic spectra of pulsed YAG laser induced plasma of A5083 in air ( $E_0=80\text{J/p}$ ,  $\tau_p=21\text{ms}$ )

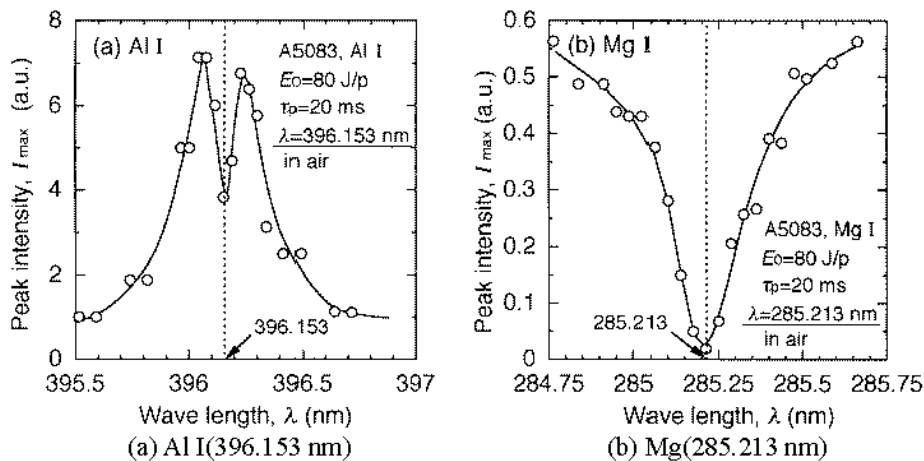


Fig.3 Intensity profile of self-absorbed lines in laser induced plasma of A5083 in air

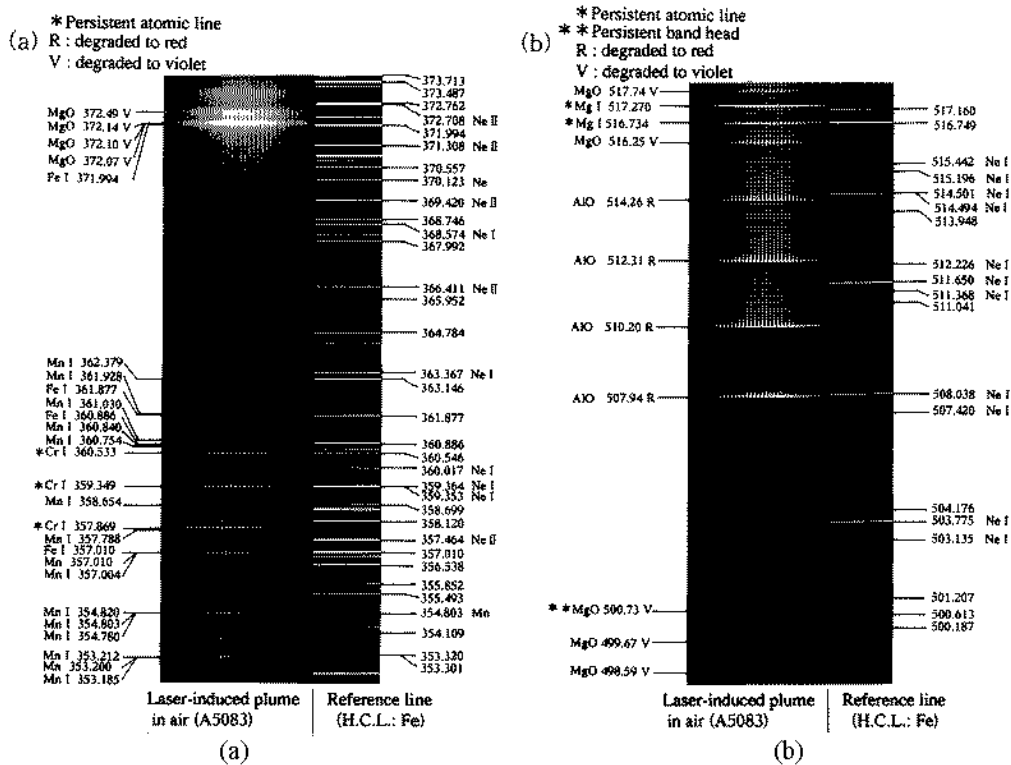


Fig.4 Atomic and molecular spectra of pulsed YAG laser induced plasma of A5083 in air ( $E_0=80\text{J/p}$ ,  $\tau_p=21\text{ms}$ )

It was clearly observed that the self-absorption took place strongly at the central wavelength of persistent line and its degree was more eminent in Mg spectral lines. Similar measurements were done in other Al alloys with different Mg content and it was confirmed that the self-absorption of Mg line became less as the Mg content was reduced. Figure 4 represents the spectrogram of the identified atomic and molecular spectra. Molecular spectra of MgO were observed in the range of 370-380 nm and near 500 nm, and atomic lines of Mn, Cr and Fe were detected in the vicinity of represents the direction of degradation of molecular spectra, showing R degraded to red side(longer wave length) and V to violet (short wave length)<sup>(10,11)</sup>. Notations of \* and \*\* show the persistent line and persistent head in atomic and molecular spectra, respectively<sup>7)</sup>. In Figure 5 is shown the spectral line intensity of AlO and MgO molecular spectra in the vicinity of 510 nm measured by multi-channel detector.

In order to confirm the original of molecular spectrum, similar measurements were conducted in the Argon shield under the same laser irradiation condition with the above stated experiments. The result showed that no molecular spectrum of AlO and MgO was observed in Argon atmosphere, and this indicated that AlO and MgO species were formed by chemical reaction of evaporated Al and Mg from pool surface with oxygen in the air. However, AlH molecular spectra were detected in the vicinity of 430 nm even in Argon atmosphere.

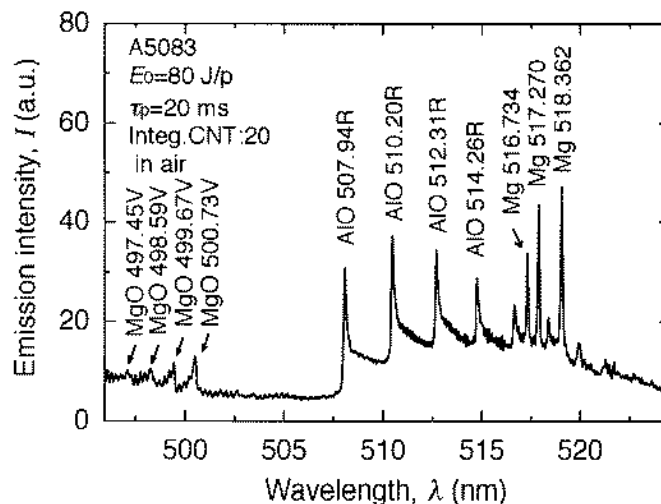


Fig.5 Molecular spectra near 510 nm measured by multi-channel detector

Figure 6 shows the spectra in the wavelength range of 420-440 nm under the different surface and shielding condition. Figure 6 (a) and (b) show the spectra of plasma induced on the Al alloy surface as received and polished condition. Due to the different in reflectivity by the surface condition, the spectrum intensities are different, but the relative intensity ratio of AlH to Cr is almost the same. While, Figure 6(c) is a case when 10 % Hydrogen is added to Argon shield under the same surface condition with Figure 6(b). The intensity of AlH molecular spectrum is much stronger than those of previous case. The formation of AlH molecular is presumed by the chemical reaction between the evaporated Al and the hydrogen or water absorbed on the surface or in the shield gas, or Hydrogen soluted in the material.

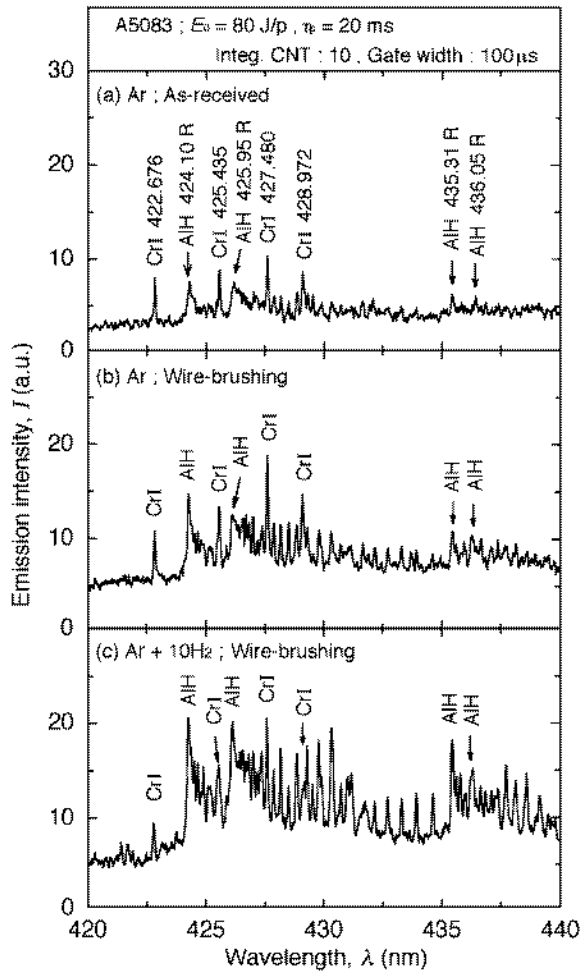


Fig.6 Effect of surface condition and ambient gas on intensity of AlH spectra

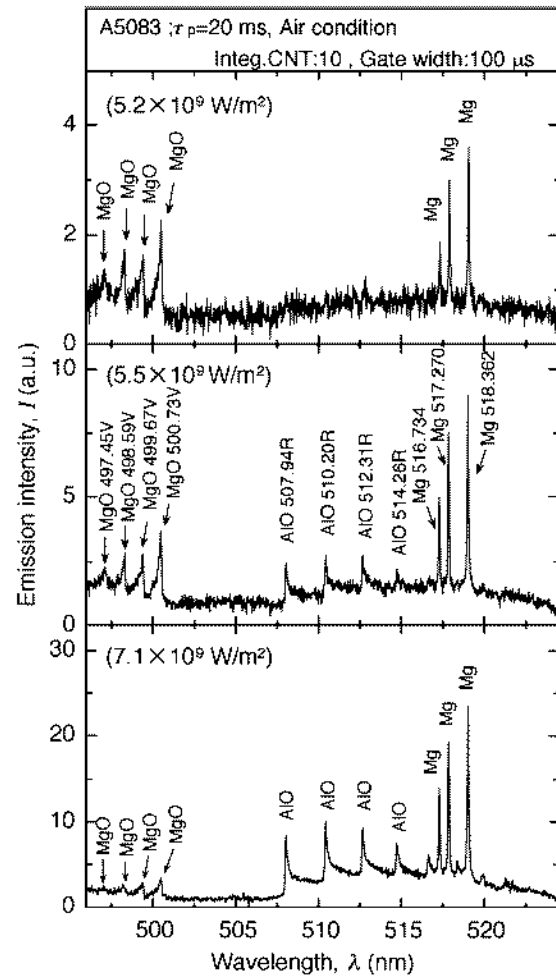


Fig.7 Effect of laser irradiation power density on intensity of molecular spectra

### 3.2 Effect of laser power density on spectrum intensity

As Aluminum alloys used in this study contain Magnesium as shown in Table 1, and Mg is more volatile than Al as indicated in Table 2, it is expected that the vaporization of Al and Mg may change depending on the surface temperature of the laser-heated molten pool. The authors analyzed the spectra species of A5083 plasma generated in air under different laser energy conditions.  $100\ \mu\text{m}$  at 2ms after laser ignition and 10 data were integrated. The results are shown in Figure 7. When laser energy was lower, i.e., lower power density condition, major species were MgO molecular spectra. However, as the laser energy was increased, MgO spectrum decreased its intensity and AlO spectra intensity increased. Figure 8 shows the intensities of AlO and MgO band spectra and their ratio as a function of input energy.

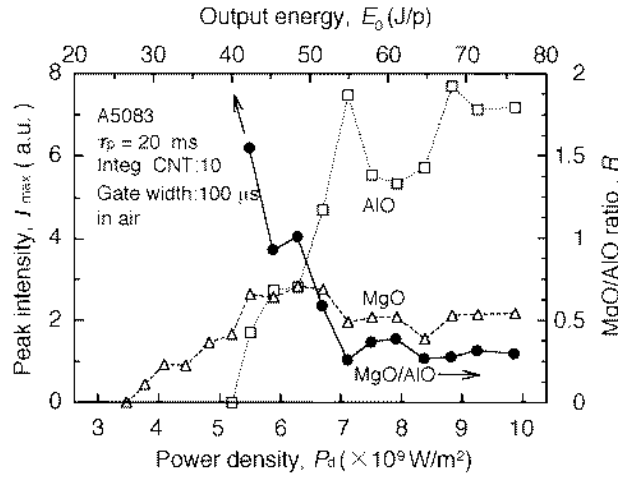


Fig.8 Variation of relative intensities of molecular spectra at 3mm high above surface as a function of laser energy

3.3 Spatial and temporal intensity distribution of spectrum

Figure 9 show the spatial distribution of spectral intensity of atomic and molecular lines. Lines selected in this experiment were persistent line and had strong intensities, as well they were quite isolated from other lines receiving little interference by other spectra. The atomic line used was Cr I ( $\lambda=428.972 \text{ nm}$ ) because it was not a self-absorption line. As seen in Figure 9(a), the intensity was strongest in the vicinity of target surface and it decreased as the distance from plate surface increased. on the contrary, the intensity of molecular spectra shown in Figure 9(b) were weak near the surface and they increased rapidly as the highest was increased. They shoe the maximum intensity at the height of around 5mm and decreased at higher place. This indicated that the evaporated Al and Mg atoms from liquid surface reacted chemically with oxygen in the air. Namely, the AlO and MgO molecular spectra were emitted by the chemical reaction of metallic atoms with oxygen in the plasma.

As described in the previously section, the evaporation of Mg species was more eminent in the low power density condition. The same phenomena were also observed in the temporal change of spectrum intensity. The intensity of MgO spectrum is very strong at the beginning and end of the laser pulse because of the lower surface temperature of liquid pool at these timing.

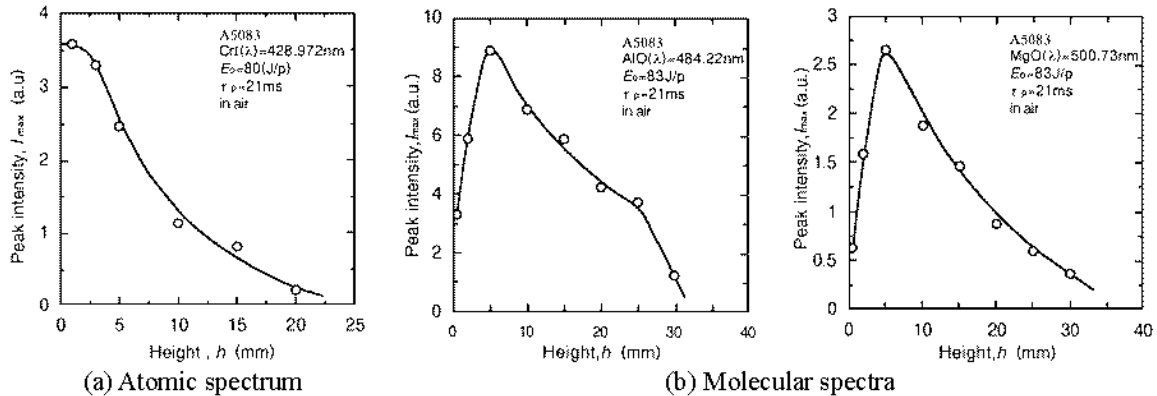


Fig. 9 Variation of spectra intensity along the plasma height

3.4 Measurement of plasma temperature and electron number density

Plasma temperature was determined by Boltzmann plot method of relative intensities measurements of several spectral lines under the assumption of local thermal equilibrium (LTE)<sup>13</sup>.

The theoretical relation to determine temperature from spectral line intensity is given as follow.

$$\ln\left(\frac{I_{nm} \lambda_{nm}}{g_n A_{nm}}\right) = -\frac{E_n}{kT} + \ln\left(\frac{N_0 hc}{Z}\right) \quad (1)$$

where,  $I_{nm}$ : spectral line intensity for  $n \rightarrow m$  level transition,  $\lambda_{nm}$ : Wave length of spectral line for  $n \rightarrow m$  level transition,  $g_n$ : Statistical weight at  $n$ -th level,  $A_{nm}$ : Transition probability for  $n \rightarrow m$  level transition,  $E_n$ :

Excitation energy to  $n$ -th level,  $k$ : Boltzmann constant,  $N_0$ : Total number density of atom,  $h$ : plank's constant,  $c$ : Velocity of light, and  $Z$ : Partition function of atom at temperature  $T$ .

Therefore, if values of  $\ln(I_{nm}\lambda_{nm}/g_n A_{nm})$  are taken in vertical axis and  $E_n$  is taken in horizontal axis for several spectral lines, the temperature can be decided from the gradient of line. In this study, atomic Cr lines were selected as shown in Table 3 because they were not self-absorbed, but sufficient intensity without any interference by other spectra.

Figure 10 shows the Boltzmann plot of 6 Cr atomic lines measured at 1mm high above the plate surface under the irradiation condition of  $E_0 = 80 \text{ J/p}$ ,  $\tau_p=21 \text{ ms}$  and the beam power density of  $1.0 \times 10^{10} \text{ W/m}^2$  at the plate surface. The data was taken 10 times and they were processed by a 100 kHz analyzer to obtain the time averaged value, and the obtained intensity was calibrated by a standard light source. The line in Fig 10 was fixed by the least square method and the plasma temperature determined from its gradient was  $3,280 \pm 150 \text{ K}$ . This values is very close to that obtained by Peeble<sup>13)</sup> ( $3,400 \pm 300 \text{ K}$ )

Table 3 Physical properties of Cr I spectra

$\lambda$ (nm)	$E_n$ (eV)	$g \cdot A(10^8/s)$
357.869	3.46	8.3
359.349	3.45	7.0
360.553	3.44	5.2
425.435	2.91	2.0
427.480	2.90	1.5
428.972	2.90	0.95

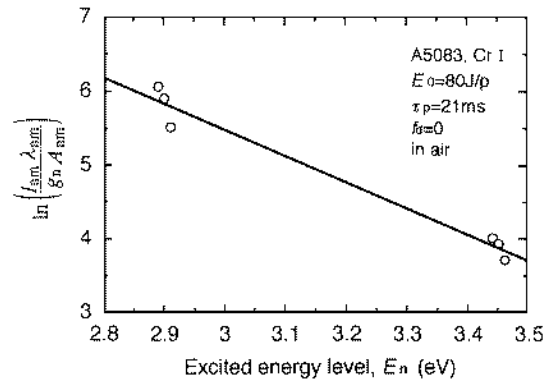


Fig.10 Boltzmann plot of 6 CrI line to determine electron temperature

The electron number density of plasma was measured by the following way. Saha's equation is given as

$$S_k = \frac{N_i N_e}{N_a} = \frac{(2\pi m_e kT)^{3/2}}{h^3} \cdot \frac{2Z_i}{Z_a} \exp\left(-\frac{V_i}{kT}\right) \tag{2}$$

where,  $S_k$ : Saha's ionization constant,  $N_a, N_i, N_e$ : number densities of atom, positive ion and electron,  $Z_a, Z_i$ : partition function of atom and ion,  $V_i$ : ionization potential, and  $T$ : temperature.

Spectra intensities of atomic line and ionic line are expressed as follows;

$$I_a = N_a \frac{g_a}{Z_a} A_a h \nu_a \exp\left(-\frac{E_a}{kT}\right) \tag{3}$$

$$I_i = N_i \frac{g_i}{Z_i} A_i h \nu_i \exp\left(-\frac{E_i}{kT}\right) \tag{4}$$

Where,  $g_a, g_i$ : Statistical weight of excited states,  $E_a, E_i$ : Transition probability,  $A_a, A_i$ : Transition probability, and  $\nu_a, \nu_i$ : Frequency of radiation.

From equation (1) to (4), one obtains the following relation.

$$N_e = \frac{I_a g_i A_i \nu_i}{I_i g_a A_a \nu_a} \cdot \frac{2(2\pi m_e kT)^{3/2}}{h^3} \exp\left(\frac{E_a - E_i - V_i}{kT}\right) \tag{5}$$

Therefore, measuring the intensities of atomic and singly ionized of the same element, one can obtain the electron number density. In this study, intensities of the MgI line of 333.668 nm and Mg II line of 280.270nm were used. The obtained electron number density at measured temperature stated previously was  $1.85 \times 10^{19} \text{ 1/m}^3$ .

#### 4. Conclusion

The major conclusions obtained in this work were as follows:

- 1) Identified spectral lines of induced plasma of Al-Mg alloys were the atomic spectra of Al, Mg, Mn, Cu, Fe and Zn, the singly ionized line of Mg, and molecular spectra of AlO, MgO and AlH. The intensity of spectra was the same with those of arc excited spectral lines in spite of short laser irradiation.

- 2) Resonant lines of Al and Mg were strongly self-absorbed which indicated that a large amount of Al and Mg were evaporated and the plasma temperature was not high enough. The self-absorption took place more strongly in the distance closer to the target surface. As Well, the self-absorption was stronger in the plasma of higher content of Mg in alloys.
- 3) Molecular band spectra of AlO and MgO were not detected in the Argon shield. The intensity of band spectra was weak in the vicinity of plate surface. but it increased quickly as the height of plasma became longer up to 5mm from the surface. In still higher position, it decreased gradually. The fact showed that the molecular spectra were emitted in the plasma by the strong chemical reactions between the evaporated metal vapors and oxygen in the air.
- 4) AlH band spectrum was detected even in the Argon shield plasma. Its intensity was strongly affected by the surface oxide layer of Al alloys as well as the Hydrogen content in the shield gas. The origin of AlH spectrum was estimated by the chemical reaction of Al vapor with Hydrogen in the shield gas or soluted in the base metal, and water adsorbed on the specimen surface.
- 5) The intensity of MgO band spectra was stronger under the condition of low power density laser irradiation, while that of AlO was predominant under the high power density irradiation condition. The similar phenomenon was observed in the temporal sequence during a single laser shot. Namely, at the beginning or end of laser shot when the pool temperature was not high, the MgO lines were much stronger than those of AlO. This was attributed by the great difference in boiling point and vaporization energy of Al and Mg.
- 6) Under the laser irradiation of  $1.0 \times 10^{10} \text{ W/m}^2$  in the air, the plasma temperature and electron number density of Al-Mg alloy were measured by spectroscopic methods, and obtained temperature was  $3280 \pm 150 \text{ K}$  and electron number density was  $1.85 \times 10^{19} \text{ 1/m}^3$ . Namely, the laser induced plasma of Al-Mg alloy was not a high temperature plasma but a very weakly ionized plasma of low temperature, slightly higher than the boiling point of Al.

#### References

- [1] J.D. Kim, Y.S Kim and A. Matsunawa : *The 1st High Energy Committee Meeting of The Korean Welding Society*, 1(2000), March, p.19.
- [2] A.Matsunawa and T. Ohnawa : *ICALEO '84*, Boston, November(1984), p.34.
- [3] C.E Moor : "Atomic Energy Level", Circular of the National Bureau of Standard 467, Vol.I, Washington(1949).
- [4] Japan Institute of Metals : "Metal Data Book 3rd Edition", Maruzen, Tokyo(1993)
- [5] G.R. Harrison : "Wavelength Table", The MIT Press, Cambridge(1969)
- [6] A.N.Zaidel, V.K. Prokofev and S. M. Raiskii : "Tables of Spectrum Lines", Pergamon Press, Berlin(1961)
- [7] R.W.B. Pearse and A.G. Gaydon : "The Identification of Molecular Spectra", Chapman and Hall Ltd., London(1976)
- [8] C.H. Corliss and W.R. Bozman : "Experimental Probabilities for Spectral Lines of Seventy Elements", NBS Monograph 53(1962)
- [9] S. Bashkin and J.O. Stoner : "Atomic Energy Levels and Grotrian Diagrams", Vol. I, North-Holland Pub. Co.(1975)
- [10] M. Singh and N.A. Narasimham : *J. Phys. B(Atom. Molec. Phys.)*, Great Britain, Ser. 2, Vol. 2, p.119,
- [11] K.P. Huber and G Herzberg : *Molecular Spectra and Molecular Structure*, IV, Constants of Diatomic Molecules, Van Nostrand Reinhold Co., New York, (1979)
- [12] H. R. Griem : "Plasma Spectroscopy", McGraw-Hill Book Co.(1964)
- [13] H. C. Peebles and R. L. Williamson : *LAMP '97*, Osaka, May(1987), High Temperature Soc. Of Japan, p.19.